Conditional Hypovascularization and Hypoxia in Islets Do Not Overtly Influence Adult β-Cell Mass or Function

Joke D'Hoker,[1] Nico De Leu,[1] Yves Heremans,[1] Luc Baeyens,[1] Kohtaro Minami,[2] Cai Ying,[1] Astrid Lavens,[1] Marie Chintinne,[1] Geert Stangé,[1] Judith Magenheim,[3] Avital Swisa,[3] Geert Martens,[1] Daniel Pipeleers,[1] Mark van de Casteele,[1] Susumo Seino,[2] Eli Keshet,[3] Yuval Dor,[3] and Harry Heimberg[1]

It is generally accepted that vascularization and oxygenation of pancreatic islets are essential for the maintenance of an optimal β-cell mass and function and that signaling by vascular endothelial growth factor (VEGF) is crucial for pancreas development, insulin gene expression/secretion, and (compensatory) β-cell proliferation. A novel mouse model was designed to allow conditional production of human sFlt1 by β-cells in order to trap VEGF and study the effect of time-dependent inhibition of VEGF signaling on adult β-cell fate and metabolism. Secretion of sFlt1 by adult β-cells resulted in a rapid regression of blood vessels and hypoxia within the islets. Besides blunted insulin release, β-cells displayed a remarkable capacity for coping with these presumed unfavorable conditions: even after prolonged periods of blood vessel ablation, basal and stimulated blood glucose levels were only slightly increased, while β-cell proliferation and mass remained unaffected. Moreover, ablation of blood vessels did not prevent β-cell generation after severe pancreas injury by partial pancreatic duct ligation or partial pancreatectomy. Our data thus argue against a major role of blood vessels to preserve adult β-cell generation and function, restricting their importance to facilitating rapid and adequate insulin delivery. *Diabetes* 62:4165–4173, 2013

Tissue recombination and misexpression experiments revealed that endothelial cells are indispensable for ontogeny of the endocrine pancreas (1). Mice devoid of *Kdr*, the vascular endothelial growth factor (VEGF) receptor type 2, lack endothelial cells and show impaired expression of *Ptf1a*, a functional marker of pancreas progenitor cells, and absence of insulin and glucagon gene expression (2). Moreover, vascular density near the branching pancreatic epithelium appears crucial for pancreatic cell type specification during development (3–5). During development, endothelial cell signaling induces VEGF-A production by β-cells, thereby further increasing islet blood vessel density and permeability (6–9). In addition, islet blood vessels provide adult β-cells with a basement membrane that is essential for β-cell proliferation as well as glucose responsiveness of insulin production and secretion (8,10).

Pdx1Cre/Vegf^fl/fl mice show decreased β-cell mass with a reduced density of insulin granules and impaired insulin gene expression and secretion, resulting in impaired glycemic control (8,11,12). *RIPCre/Vegf*^fl/fl mice possess normal β-cell mass but show a retarded glucose clearance and decreased glucose-induced insulin release (7,9), while insulin secretion from perifused transgenic islets was accelerated compared with wild-type islets (9). The above models unfortunately lack temporal control and can therefore not distinguish between the effects of VEGF signaling on β-cell mass and function in adult pancreas from those provoked in the developing pancreas. The current study describes a novel, conditional transgenic model to induce islet vessel regression to investigate the genuine role of the islet vasculature of adult mice with regard to β-cell mass and function.

RESEARCH DESIGN AND METHODS

Rat insulin promoter (RIP)-rtTA (13,14) and TetO-*sFLT1* (4,15) mice (both on a mixed background, mainly ICR [CD1]) were 8–12 weeks old. Experiments were in accordance with the guidelines of our institutional Ethical Committee for Animal Experiments and with the national guidelines and regulations. Genotyping was performed using the following primers: RIPrtTA: 5′-TAGATGTGCTTTACTAAGTCATCGCG-3′ and 5′-GAGATCGAGCAGGCCCTC GATGGTAG-3′; TET-sFLT1: 5′-CGACTCACTATAGGGAGACCC-3′ and 5′-TGG CCTGCTTGCATGATGTG-CTGG-3′. Doxycline (DOX) was administered through the food (625 mg/kg; Harlan Laboratories, Boxmeer, the Netherlands). Tail vein blood glucose level and body weight were evaluated between 10:00 and 12:00 A.M., with or without prior fasting (overnight or 2 h), as indicated. Intraperitoneal glucose tolerance tests were performed by injecting glucose (2 g/kg body wt i.p.) after an overnight fast. Mouse islets were isolated from transgenic mice by intraductal injection of 0.3 mg/mL collagenase type XI (Sigma, St. Louis, MO). Handpicked islets were dissociated with trypsin, and β-cells were sorted on the basis of size and flavin adenine dinucleotide content. 80% of the resulting cell preparation consisted of β-cells, as determined by immunostaining for insulin. Sustained-release insulin implants (LinBit, LinShin, Toronto, Canada) (1 implant per mouse) were implanted subcutaneously under the mid-dorsal skin. Partial pancreatic duct ligation (PDL) and partial (60%) pancreatectomy (PPx) were performed as previously described (16,17).

RNA and protein analysis. Total RNA was isolated from tissue (TRIzol; Life Technologies, Carlsbad, CA), from islets (RNeasy; Qiagen, Venlo, the Netherlands), or from cells (PicoPure; Life Technologies). Only RNA with RNA integrity number ≥7 was retained for analysis. cDNA synthesis and RT–quantitative PCR was done as described (18). Quantitative PCR was performed using mouse-specific Assays on Demand (Applied Biosystems, Life Technologies) (see Supplementary Table 1) with TaqMan Universal PCR master mix on an ABI Prism 7700 Sequence Detector, and data were analyzed using the Sequence Detection Systems Software, version 1.9.1 (all Applied Biosystems). For avoidance of interference from contaminating genomic DNA, primer sets were designed to span at least one intron. Expression levels were normalized to the expression level of the housekeeping gene *Ppia*.

For primary antibodies used, see Supplementary Table 2. Secondary antibodies were cyanine-labeled (Jackson ImmunoResearch, Newmarket, U.K.). Nuclei were labeled with Hoechst 33342. GLUT2 was detected using an

ImmPRESS Polymer Detection kit (Vector Laboratories, Burlingame, CA). Sections were imaged using a Zeiss Axioplan 2 microscope. Scale bars are 100 μm. The measurement of β-cell mass and β-cell mass distribution according to endocrine cluster size was performed as previously described (19). For quantitation of β-cell proliferation, percentages of Ki67-positive β-cells were measured as mean ± SEM. For all conditions, at least 1,500 β-cells were counted. Insulin content of pancreas was determined with a mouse insulin RIA kit (Linco Research, St. Charles, MO). Insulin release by islets (20 freshly isolated islets per condition) was measured after preincubation in Ham F10 medium without glucose for 2 h at 37°C and 5% CO₂ and incubation for 2 h in Ham F10 medium containing 2 mmol/L Ca²⁺ and either 2 mmol/L (G2), 10 mmol/L (G10), or 20 mmol/L (G20) glucose. Insulin content of medium and cells was measured with a mouse insulin RIA kit (Linco Research). β-Cell area was determined by morphometric analysis on E-cadherin/insulin-stained slides using ImageJ. Relative amount of α-cells was evaluated by expressing the glucagon-positive area as percentage of total islet area, calculated as sum of insulin- and glucagon-positive areas.

Measurement of vascularization and hypoxia. Functional vessels were labeled by intravenous injection of biotinylated tomato lectin (Lycopersicon esculentum; Vector Laboratories) (20). Five minutes after injection, intravenous blood cells were flushed from the circulation of anesthetized mice by systemic perfusion with PBS, followed by overnight fixation of the samples at 4°C with 10% (vol/vol) neutral-buffered formalin prior to paraffin embedding and sectioning. Tomato lectin was visualized with Alexa Fluor 555–labeled streptavidin (Life Technologies). Intraislet vessel density was calculated by morphometric analysis using IPLab Pathway 4.0 for PC (BD) and represents the proportion of the amount of tomato lectin–positive vessels per islet area (number of vessels × 1,000 per number of insulin-positive pixels). For detection of hypoxia, the oxygenation marker pimonidazole (60 mg/kg body wt i.p.; HPI, Burlington, MA) was injected. One hour after injection, the animals were anesthetized, followed by systemic perfusion during 10 min with 10% (vol/vol) neutral-buffered formalin. Organs were embedded in paraffin without postfixation, sectioned, and reacted with a mouse anti–hypoxyprobe-1 antibody (HPI) after heat-mediated antigen retrieval using 0.1 mol/L glycine, pH 9.0. Chromogenic detection was done with an EnVision+ kit (Dako) according to manufacturer's instructions.

Pancreas perfusion. Perfusion of mouse pancreases was performed as previously described (21). Briefly, mice were fasted overnight. Pancreata were perfused at 1 mL/min during 10 min with Krebs-Ringer bicarbonate (KRB) HEPES buffer containing 2.8 mmol/L glucose, followed by 15 min perfusion with KRB buffer containing 16.7 mmol/L glucose and ending with KRB buffer containing 2.8 mmol/L glucose. Insulin in the perfusate was measured by the homogeneous time-resolved fluorescence–based assay (CIS Bio International, Gif sur Yvette, France).

Glucose oxidation and utilization. For measurements of glucose oxidation and utilization, batches of 15 islets were incubated in KRB HEPES/0.25% (wt/vol) BSA containing 1 μCi D-[U-¹⁴C]glucose/5 mL (300 mCi/mmol) and 1 μCi D-[5-³H]glucose/mL (13.5 Ci/mmol) at 2.5, 10, and 20 mmol/L glucose for 2 h. Glucose oxidation was measured by the generation of KOH-trapped ¹⁴CO₂, and glucose utilization was determined by measuring the amount of ³H₂O generated as previously described (22).

Electron microscopy. Samples were fixed in 2.5% (vol/vol) glutaraldehyde in 0.1 mol/L sodium cacodylate buffer, pH 7.4, postfixed in 1% (wt/vol) osmium tetroxide, stained with 2% (wt/vol) uranyl acetate, and embedded in Spurr resin, and ultra-thin plastic sections were examined with a ZEISS EM 9S2 electron microscope.

Data analysis. Values are depicted as mean ± SEM from at least three independent experiments and considered significant when $P \leq 0.05$. Data were statistically analyzed by (un)paired Student t test, one-way ANOVA with Bonferroni posttest, or one-sample t test as indicated (GraphPad Prism, version 5.0b [http://www.graphpad.com]).

RESULTS

sFLT1 overexpression in β-cells severely reduces the islet vascular network.

Double transgenic (dTG) mice were generated by crossing driver mice that express reverse tetracycline *trans*-activator (rtTA) under the control of the RIP with responder mice that express human *sFLT1* when rtTA binds to the operator sequence (TetO) in the presence of tetracycline or DOX (Fig. 1*A*). β-Cells from these double transgenic mice thus conditionally produce human soluble Flt1 (sFlt1), a splice variant of the VEGF receptor 1 (*Flt1*) that binds extracellular VEGF or PlGF and thereby antagonizes their signaling (15). Since β-cells
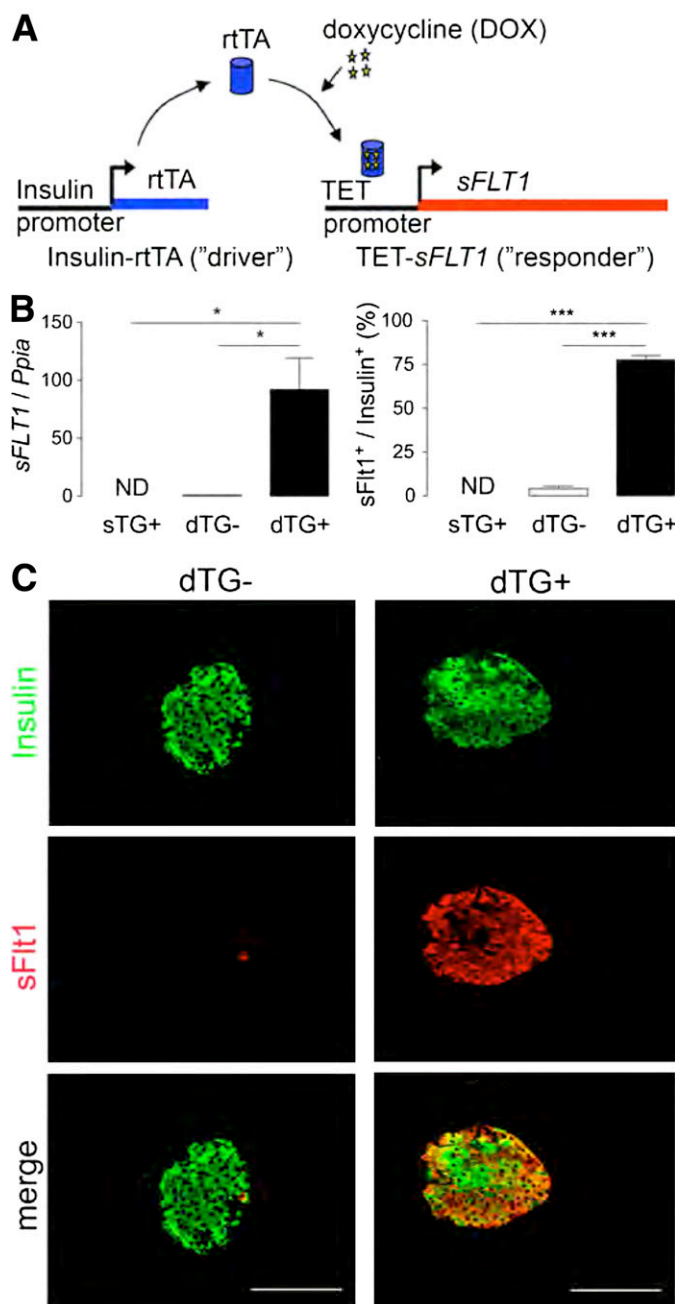
FIG. 1. Efficient overexpression of *sFLT1* in β-cells of dTG+DOX²ᵂ mice. *A*: Schematic illustration of the RIPrtTA × TetO-*sFLT1* model. *B*: DOX induces efficient *sFLT1* overexpression in β-cells of dTG mice. *Left panel*: *sFLT1* transcript level is increased in islets, isolated from dTG+DOX (dTG⁺) mice (*n* = 3; result expressed relative to expression level in dTG-DOX mice [dTG⁻]). *Right panel*: Percentage of β-cells that produce sFlt1 is increased in dTG+DOX mice (*n* = 3–4). *C*: sFlt1 (red) is specifically overproduced in β-cells (insulin [green]) of dTG+DOX mice. All analyses were done after 2 weeks ± DOX. Data were statistically analyzed by one-way ANOVA with Bonferroni posttest. *P ≤ 0.05, ***P ≤ 0.001. ND, nondetectable.

attract blood vessels by releasing VEGF (11), we hypothesized that the high local levels of sFLT1, produced and secreted by β-cells, would interfere with the cross-talk between β- and endothelial cells and might thereby reduce islet vascularization and, presumably, oxygenation. To test the specificity and efficacy of *sFLT1* expression/production, 8- to 12-week-old RIPᵗᵗᵀᴬTetOˢᶠᴸᵀ¹ dTG or TetOˢᶠᴸᵀ¹ single
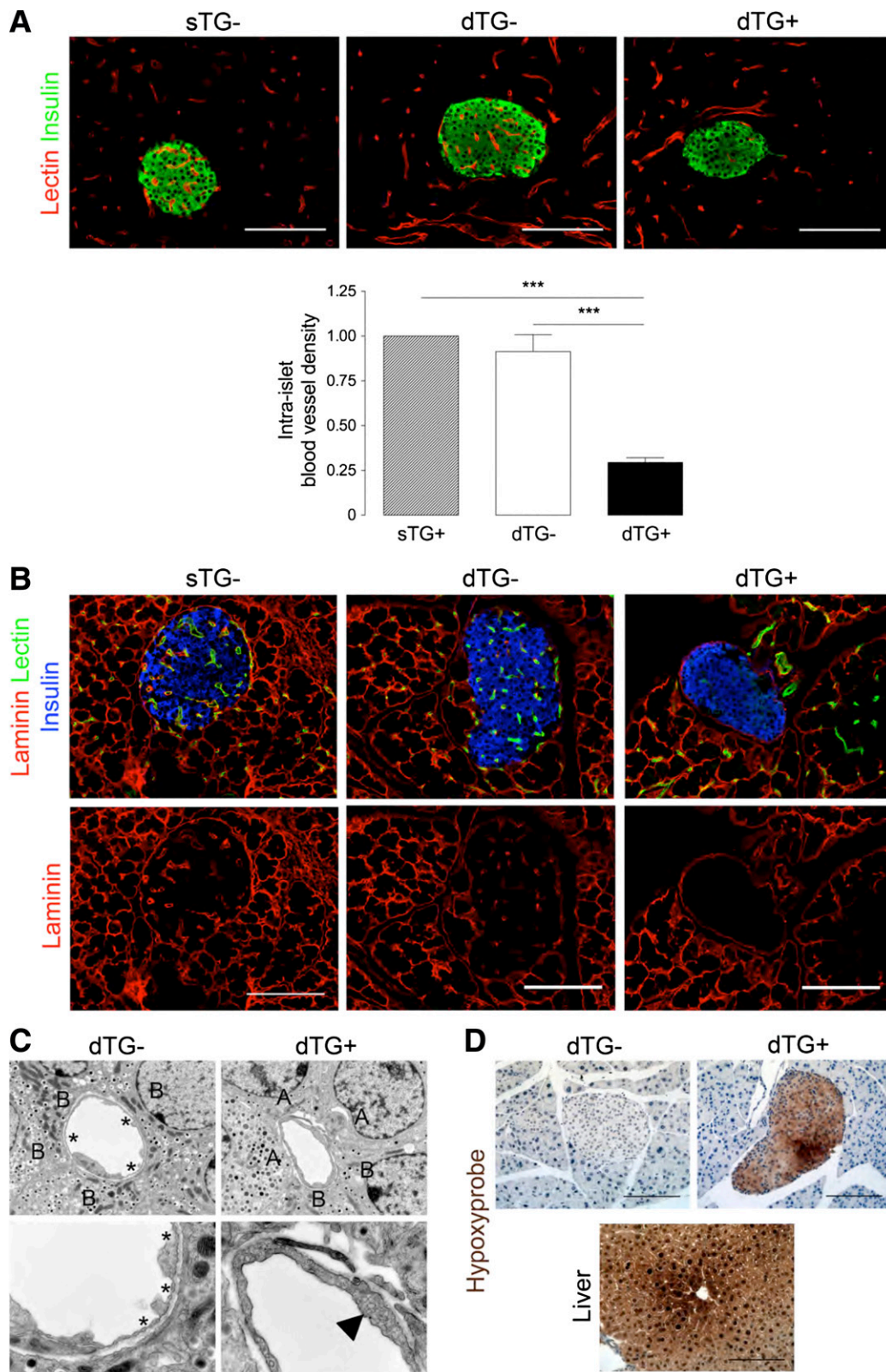
FIG. 2. Overexpression of *sFLT1* in β-cells leads to islet hypovascularization, altered islet structure, and islet hypoxia. *A, upper panel*: Pancreas sections stained for the functional vessel marker lectin (red) and insulin (green). *Lower panel*: Intraislet vessel density is reduced in dTG+DOX mice (*n* = 9). Intraislet vessel density represents the proportion of the amount of tomato lectin–positive vessels per islet area (number of vessels × 1,000 per number of insulin-positive pixels). *B*: Reduction of vascular basement membrane (laminin [red]) in dTG+DOX mice. Functional vessels are stained with lectin (green) and β-cells with insulin (blue). *C*: Thickening of the endothelial lining and absence of fenestrae (indicated with asterisks) in dTG+DOX mice. Note the increased prevalence of plasma membrane invaginations (caveolae, arrowhead) and the predominance of α-cells surrounding the depicted blood vessel in the dTG+DOX condition (*upper right panel*). A, α-cell; B, β-cell. *D*: Hypovascularization induces islet hypoxia in dTG+DOX mice. Pancreas sections stained with antibody against hypoxyprobe (pimonidazole) (brown). Liver from the same animals served as positive control. All analyses were performed after 2 weeks ± DOX. Data were statistically analyzed by one-way ANOVA with Bonferroni posttest. ***P ≤ 0.001.

transgenic (sTG) mice were fed DOX-containing chow during 2 weeks (DOX^{2W}). Under these conditions, the transcript encoding *sFLT1* was significantly induced (Fig. 1*B*), resulting in production of sFlt1 protein by the majority of β-cells (Fig. 1*B* and *C*) and a decrease of 68% compared with dTG$^-$ and of 71% compared with sTG$^+$ of functional intraislet vessels compared with sTG-DOX^{2W} and dTG+DOX^{2W} control mice (Fig. 2*A*). In parallel, laminin and collagen IV, two major components of the vascular basement membrane in islets (8,10), were nearly absent after 2 weeks of DOX treatment, while the peripheral islet basement membrane remained intact (Fig. 2*B* and Supplementary Fig. 1). Given the near-identical phenotype of sTG+DOX^{2W} and dTG-DOX^{2W} mice, only dTG-DOX^{2W} mice were used as control from then on.

Compared with control mice, very few fenestrae were detected in the few remaining intraislet endothelial cells in dTG+DOX^{2W} mice, while they contained an increased number of plasma membrane invaginations (caveolae) (Fig. 2*C*).

Moreover, these endothelial cells were predominantly surrounded by α- rather than by β-cells (Fig. 2*C*).

Intraislet hypoxia was evaluated by intravenous injection of pimonidazole that precipitates at oxygen levels of ≤8 mmHg (23). Islets from dTG+DOX^{2W} mice stained positive for pimonidazole with medium/large islets (>100 μm diameter) displaying more pimonidazole$^+$ cells than small islets (<100 μm diameter) (29.0 ± 2.4% in <100 μm vs. 46.4 ± 7.0% in >100 μm) (n = 4). The intensity of pimonidazole staining was more heterogeneous in medium/large islets and inversely related to the distance toward the most proximate blood vessel (Fig. 2*D* and Supplementary Fig. 2). Whether pimonidazole precipitation associated with functionally important and metabolically relevant hypoxia was evaluated by analysis of transcripts encoding *Hif1a/Vegfa* and glycolytic enzymes in islets isolated from dTG+DOX^{2W} mice. Although HIF1a protein could be observed in the nuclei of islet cells, neither *Hif1a* nor *Vegfa* mRNA levels
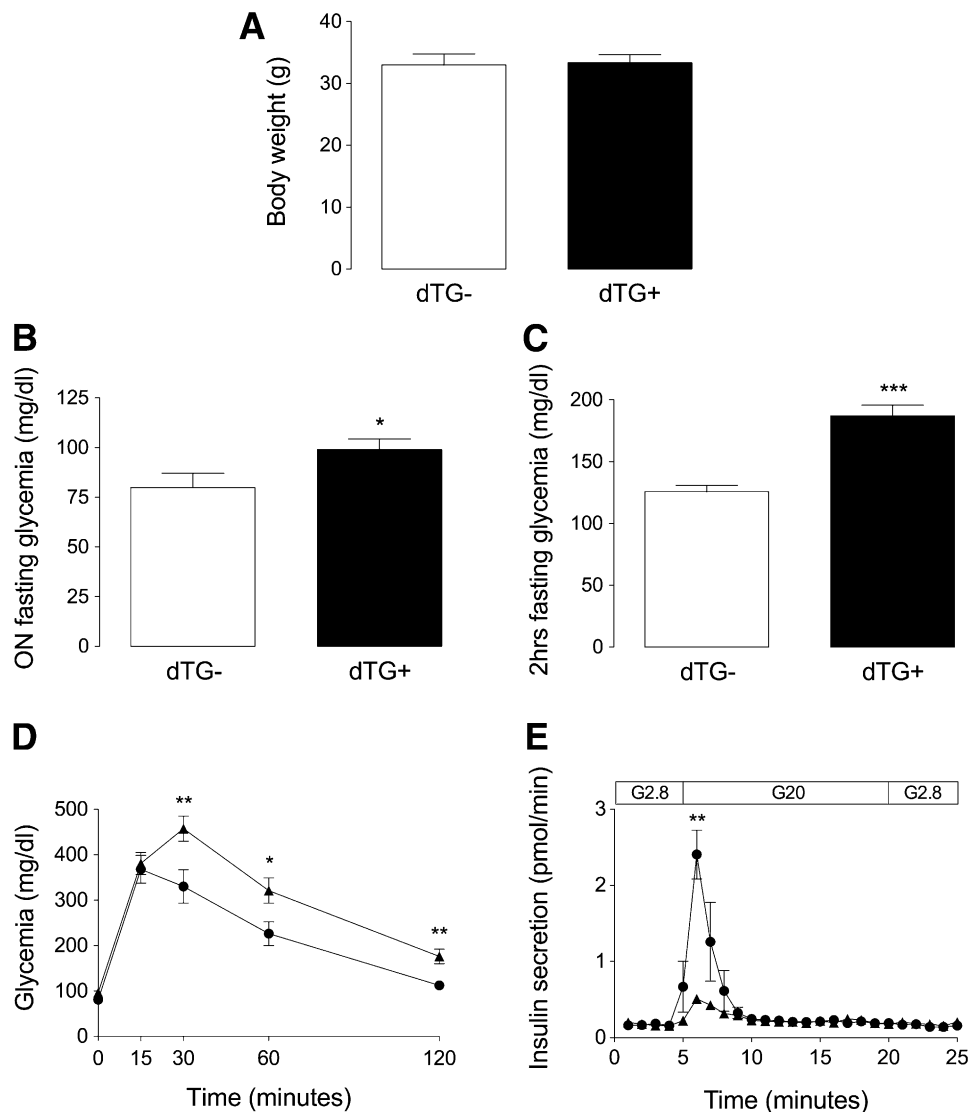
FIG. 3. Islet hypovascularization and hypoxia results in impaired fasting glucose and blunted glucose-stimulated insulin secretion with subsequent impaired glucose tolerance. *A*: Body weight is unchanged in dTG+DOX mice (n = 5). *B* and *C*: Overnight (n = 15) (*B*) and 2-h (*C*) fasting glycemia (n = 8) is increased in dTG+DOX mice. *D*: Impaired glucose tolerance in dTG+DOX mice (n = 11). *E*: In vivo pancreas perfusion (n = 4). Glucose-stimulated insulin release is blunted in dTG+DOX mice. All analyses were done after 2 weeks ± DOX. Data were statistically analyzed by unpaired *t* test. *$P \leq 0.05$, **$P \leq 0.01$, ***$P \leq 0.001$. hrs, hours; ON, overnight.

were significantly altered 2 weeks after sFlt1-mediated vessel ablation. Expression of *Flt1* (*VEGFR1*), *Kdr* (*VEGFR2*), and *Flt4* (*VEGFR3*) was significantly reduced in DOX^{2W}-treated animals, coinciding with the observed vessel regression (Supplementary Fig. 3*A*). Immunostaining showed an increased amount of nuclear HIF1-α, a similar level of VEGF, and a severe decrease in KDR and FLT4 in dTG+DOX^{2W} mice (Supplementary Fig. 3*B*). Transcript levels of glyceraldehyde 3-phosphate dehydrogenase (*Gapdh*), phosphoglycerate kinase 1 (*Pgk1*), pyruvate dehydrogenase kinase 1 (*Pdk1*), and phosphofructokinase 1 (*Pfk1*) only marginally increased (% increase vs. dTG-DOX: *Gapdh*, 37.3 ± 4.1%; *Pgk1*, 30.0 ± 4.7%; *Pdk1*, 26.0 ± 14.0%; and *Pfk1*, 8.9 ± 4.3% [all $n = 3$]) In line with the absence of increased *Hif1a* and *Vegfa* gene expression, no significant differences in expression of the HIF1a downstream targets lactate dehydrogenase A (*Ldha*) or DNA-damage-inducible transcript 4 (*Ddit4*) were observed (Supplementary Fig. 4). Taken together, time-controlled and β-cell–specific overexpression of *sFLT1* results in severe islet hypovascularization but only mild hypoxia and subtle changes in the expression of glycolytic and hypoxia-regulated genes.

Hypovascularization and hypoxia impair fasting glucose and blunt glucose-stimulated insulin release but do not overtly influence isolated β-cell function. For examination of the effect of islet hypovascularization on glucose homeostasis, blood glucose was measured after overnight and/or 2-h fasting in dTG ± DOX mice after 2 (dTG ± DOX^{2W}) or 25 (dTG ± DOX^{25W}) weeks of DOX treatment. While, at both time points, body weight did not differ between both experimental conditions (Fig. 3*A*), blood glucose level was only marginally elevated in dTG +DOX mice after overnight fasting but was more severely increased after 2 h of fasting (overnight fasting, 79.8 ± 7.3 mg/dL [$n = 15$] in dTG-DOX^{2W} vs. 100.1 ± 5.9 mg/dL in dTG+DOX^{2W} [$n = 15$] ($P ≤ 0.05$); 2-h fasting, 125.8 ± 5.1 mg/dL ($n = 8$) in dTG-DOX^{2W} vs. 179.8 ± 9.0 mg/dL in dTG+DOX^{2W} ($n = 8$) ($P ≤ 0.005$); and 2 h-fasting, 140.8 ± 6.7 mg/dL ($n = 4$) in dTG-DOX^{25W} vs. 190.0 ± 12.9 mg/dL in dTG+DOX^{25W} ($n = 4$) ($P ≤ 0.05$) (Fig. 3*B* and *C* and Supplementary Fig. 5). Similarly, rapid glucose clearance was impaired upon intraperitoneal glucose administration in dTG+DOX^{2W} mice (glycemia after 2-h intraperitoneal glucose tolerance test: 112.3 ± 6.6 mg/dL [dTG-DOX^{2W}] vs. 181.0 ± 18.6 mg/dL [dTG+DOX^{2W}]) ($P ≤ 0.05$; $n = 11$) (Fig. 3*D*). For determination of whether this glucose intolerance was caused by defective glucose-stimulated insulin release in vivo, pancreases were perfused with 20 mmol/L glucose, showing a dramatic decrease in first-phase insulin secretory response from hypovascular, hypoxic islets (Fig. 3*E*).

The possibility of intrinsic defects in glucose handling by hypovascular and hypoxic β-cells as a cause for the differences in glucose homeostasis was evaluated by analysis of transcripts coding for Glut type 1/2 (*Slc2a1* and *Slc2a2*, respectively) and glucokinase (*Gck*) and by analysis of in vitro glucose utilization and oxidation. Although Glut1 expression increased by 58% and Glut2 and glucokinase expression decreased by 31 and 23%, respectively, in hypovascular islets (Fig. 4*A* and *B*), in vitro glucose utilization and oxidation were similar, with the exception of a significant increase in glucose utilization at 20 mmol/L glucose in islets, isolated from DOX-treated animals (Fig. 4*C* and *D*). Surprisingly, insulin gene expression and total pancreas insulin content remained unaffected (78.80 ± 13.79 pg insulin/mg tissue in dTG-DOX^{2W} vs. 65.87 ± 10.46 pg insulin/mg tissue in dTG+DOX^{2W} ($n = 5$, $P = 0.48$) (Fig.
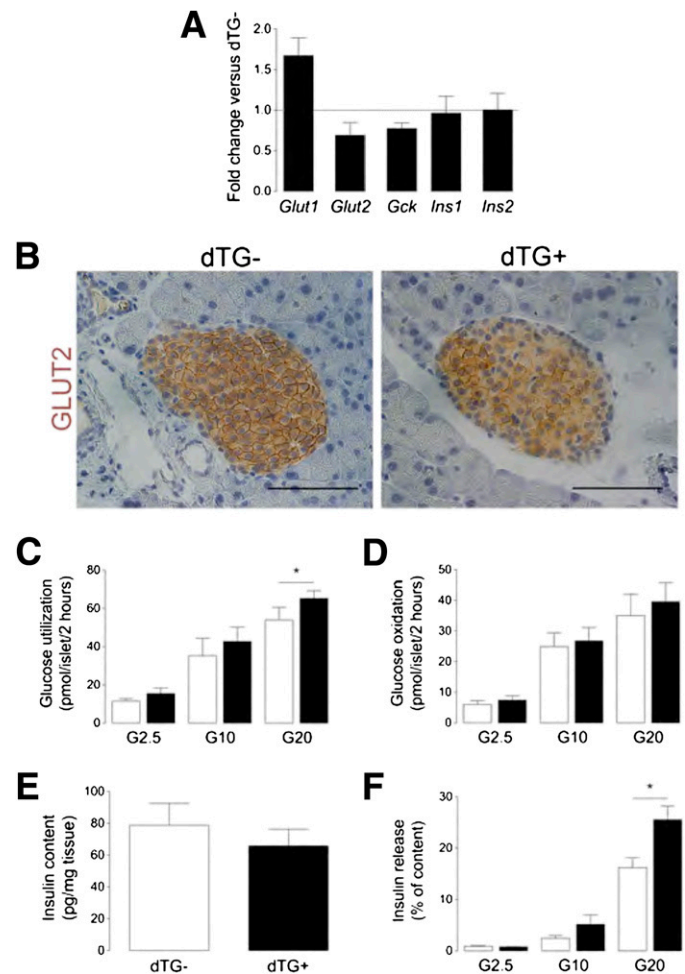
FIG. 4. Islet hypovascularization and hypoxia do not overtly influence β-cell function. *A*: Transcript level is increased for *Slc2a1* (Glut1) ($n = 3$), decreased for *Slc2a2* (Glut2) ($n = 4$) and glucokinase (*Gck*) ($n = 4$), and unchanged for insulin (Ins1/2) ($n = 3$) in islets, isolated from dTG+DOX mice. Results are expressed relative to their expression level in dTG-DOX islets, which is set at 1. *B*: Pancreas sections stained for GLUT2, illustrating decreased membrane expression of GLUT2 in dTG+DOX mice. *C* and *D*: In vitro glucose utilization ($n = 5$) (*C*) and oxidation ($n = 5$) (*D*) are unchanged in islets, isolated from dTG+DOX mice, except for an increase in glucose utilization at 20 mmol/L glucose. *E*: Pancreas insulin content ($n = 5$) is unchanged in dTG+DOX mice. *F*: Insulin release from β-cells, isolated from dTG+DOX mice, is increased at 20 mmol/L glucose (results are expressed as % of total insulin content) ($n = 4$). All analyses were done after 2 weeks ± DOX. Data were statistically analyzed by one-sample *t* test (*A*) or by (un)paired *t* test (*B–F*). G2.5, 2.5 mmol/L glucose; G10, 10 mmol/L glucose; G20, 20 mmol/L glucose. **P ≤ 0.05*.

4*A* and *E*), while glucose-stimulated insulin secretion by hypovascular, hypoxic islets demonstrated a significant increase at 20 mmol/L (Fig. 4*F*).

Taken together, these data indicate that islet hypovascularization and hypoxia correlate with increased fasting glucose, blunted glucose-stimulated insulin release, and impaired glucose tolerance in vivo but do not irreversibly influence β-cell function in isolated β-cells.

Hypovascularization and hypoxia do not influence β-cell proliferation or mass. Since both VEGF signaling and vascular basement membrane proteins have been claimed to be instrumental for proper β-cell formation and postnatal proliferation by nonconditional models of VEGF ablation (1,8), we evaluated the effect of spatiotemporal ablation of the endothelium and associated basement

membrane on β-cell proliferation and mass after 2 and 25 weeks of *sFLT1* overexpression. Interestingly, β-cell proliferation was independent of *sFLT1* overexpression and of glycemia that was normalized by an insulin-releasing implant ($0.5 \pm 0.1\%$ Ki67$^+$insulin$^+$ cells in dTG $\pm$ DOX^{2W} [$n = 11$], $0.4 \pm 0.1\%$ in dTG+DOX$^{2W+INS\ pellet}$ [$n = 6$], $0.4 \pm 0.1\%$ in dTG-DOX^{25W} [$n = 9$], and $0.3 \pm 0.1\%$ in dTG+DOX^{25W} [$n = 8$] mice) ($P > 0.05$ for comparison of all conditions) (Fig. 5A and Supplementary Fig. 6). β-Cell proliferation was not increased in small compared with large islets of dTG+DOX$^{2W\ and\ 25W}$ mice (Supplementary Table 3). In addition, β-cell mass was similar in dTG $\pm$ DOX$^{2W\ and\ 25W}$ mice (2.2 ± 0.2 mg in dTG $\pm$ DOX^{2W} [$n = 4$; $P > 0.5$], 3.2 ± 0.5 mg in dTG-DOX^{25W}, and 3.3 ± 0.5 mg in dTG+DOX^{25W} mice [$n = 4$; $P > 0.5$]) (Fig. 5B). For determination of whether islet hypovascularization influenced β-cell area or islet size, β-cell surface was measured and islets were classified on the basis of their size. No differences in surface area per β-cell or in islet size were found between dTG $\pm$ DOX^{2W} mice (Fig. 5C and E). In contrast, β-cell size was smaller in dTG+DOX^{25W} mice. The decreased β-cell size likely contributes to the increased number of small islets (12–100 μm in diameter) in dTG+DOX^{25W} mice (Fig. 5D and E). While islet cell composition was similar in medium- and larger-sized islets, the number of α-cells increased by 69% in small islets of dTG+DOX^{25W} (Fig. 5F). Despite these subtle differences in β-cell area, islet size, and islet composition, these data suggest that the islet endothelium and the associated basement membrane proteins

are dispensable for postnatal β-cell proliferation and β-cell mass expansion under normal physiological conditions.

Hypovascularization and hypoxia do not influence injury-induced increase of β-cell proliferation. Since islet hypovascularization and hypoxia exerted only minor effects on β-cell function and mass under normal physiological conditions, we evaluated whether the islet endothelium was necessary for injury-induced β-cell proliferation (16,17). DOX was administered for 7 or 14 days, respectively, immediately after injury by 60% PPx or partial PDL. Two weeks after PDL, the number of sFlt1-producing β-cells was significantly increased in DOX^{2W} animals (Supplementary Fig. 7), associated with hypovascularization and regression of the vascular basement membrane (Supplementary Fig. 8). Despite these structural changes, β-cell proliferation was similar in PDL pancreas of dTG $\pm$ DOX^{2W} mice ($1.8 \pm 0.3\%$ in dTG$^-$ vs. $2.2 \pm 0.3\%$ in dTG$^+$ [$n = 6$]) (Fig. 6A and C). Similarly, 1 week after PPx, no differences in β-cell proliferation were observed between dTG $\pm$ DOX^{1W} mice ($4.5 \pm 0.6\%$ in dTG$^-$ vs. $5.3 \pm 0.2\%$ in dTG$^+$ [$n = 4$]) (Fig. 6B and C). These data therefore do not imply a role for the islet endothelium or of its basement membrane in PDL- or PPx-mediated β-cell generation.

DISCUSSION

Islets of Langerhans are highly vascularized mini-organs (1,8,11) in which β-cells are arranged in a rosette-like pattern around blood vessels (24,25). This structural
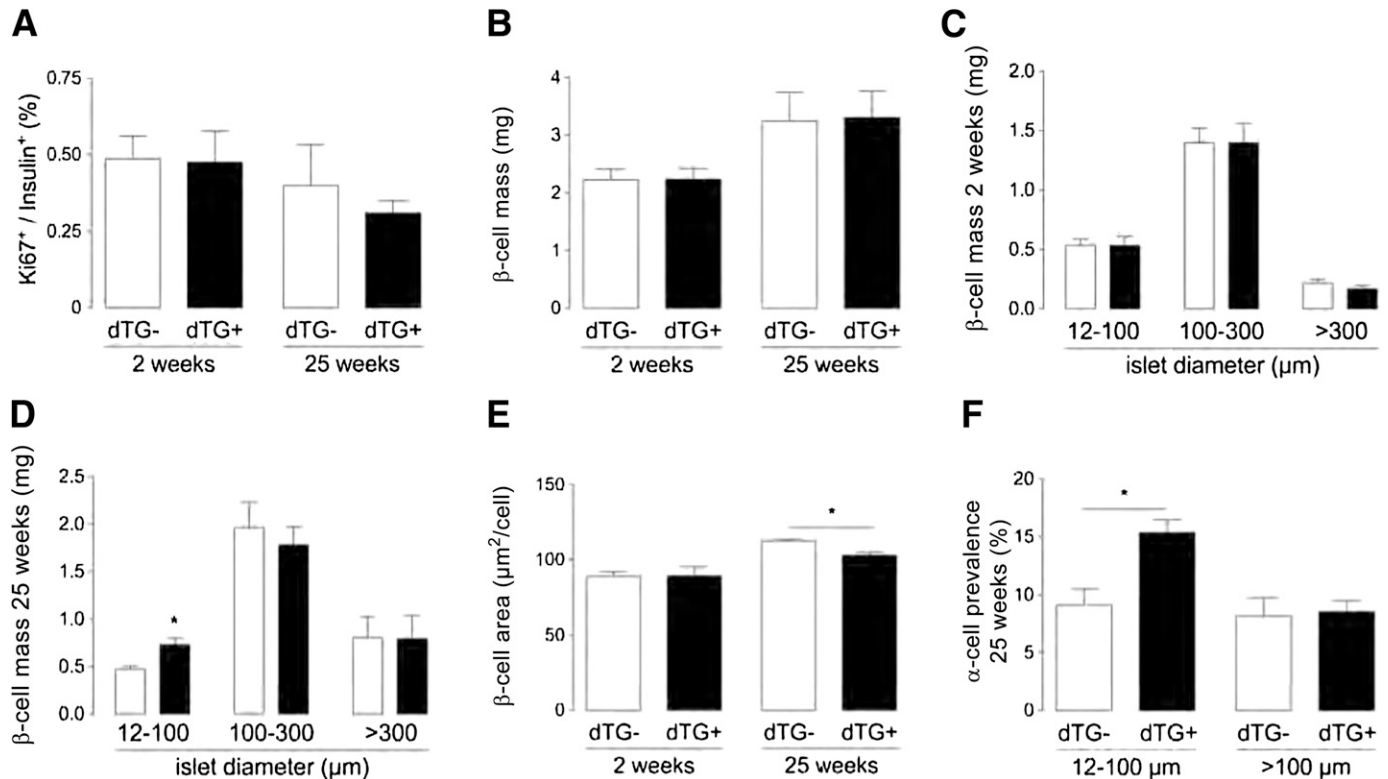
FIG. 5. Islet hypovascularization and hypoxia do not influence maintenance or growth of adult β-cells. *A–E*: β-Cell proliferation after 2 weeks (*n* = 11) and 25 weeks (*n* = 4) (*A*), β-cell mass after 2 weeks (*n* = 4) and 25 weeks (*n* = 4) (*B*), islet size after 2 weeks (*n* = 4) (*C*) and 25 weeks (*n* = 4) (*D*), and β-cell area after 2 weeks (*n* = 10) and 25 weeks (*n* = 3) (*E*) are unchanged in dTG+DOX mice except for an increase in small islets (12–100 μm diameter) (*D*) and a decrease in β-cell area in dTG+DOX mice after 25 weeks (*E*). *F*: α-Cell prevalence, measured as ratio of glucagon-positive area over (glucagon + insulin)-positive area, is increased in small islets of dTG mice after 25 weeks of DOX treatment (*n* = 4). Data were statistically analyzed by unpaired *t* test. **P ≤ 0.05.*
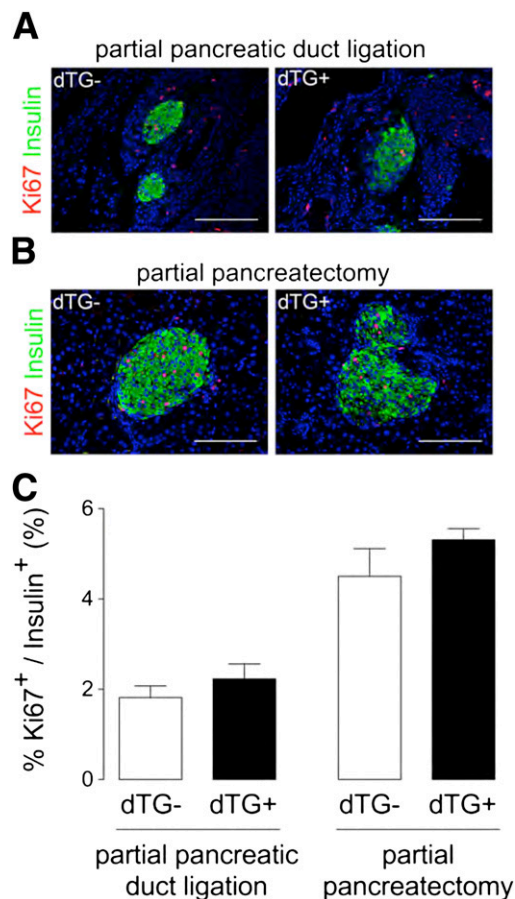
FIG. 6. Islet hypovascularization and hypoxia do not influence injury-induced β-cell proliferation. *A* and *B*: Pancreas sections from partial duct-ligated (*A*) or partial pancreatectomized (*B*) dTG mice stained for Ki67 (red) and insulin (green). *C*: β-Cell proliferation is similar in duct-ligated (*n* = 6) and partial pancreatectomized (*n* = 4) dTG+DOX compared with duct-ligated or partial pancreatectomized dTG-DOX mice. All analyses were done 2 weeks after PDL or PPx ± DOX. Data were statistically analyzed by unpaired *t* test.

organization is suggestive for the importance of endothelial-endocrine cross-talk. Indeed, endothelial cells are indispensible for proper endocrine development (1,2), while β-cells attract endothelial cells by secreting and releasing VEGFA (7–9,11). The role of VEGF and the islet endothelium has been studied in mice with *Vegf* knockout in PDX1⁺ (6,8) or insulin⁺ cells (7,9). Depletion of VEGF already during the ontogeny of these mice excludes the study of postnatal effects of VEGF on β-cell function and mass. To circumvent this caveat and determine the genuine role of endothelial–β-cell cross-talk on adult β-cell function and mass, we generated a β-cell–specific, DOX-inducible genetic system in which a secreted VEGF-trap (sFlt1) specifically interfered with VEGF signaling near β-cells of 8- to 12-week-old mice.

Impaired VEGF signaling in adult islets significantly decreased islet vessel density within 14 days. While the peri-islet basement membrane remained intact, intraislet vessel regression was associated with a loss of the vascular basement membrane. The few remaining vessels mainly associated with α-cells and displayed, in line with the observations from others (11), very few fenestrae and a high number of plasma membrane invaginations (caveolae). This observation indicates that islet blood vessels require

continuous VEGF signaling for their maintenance and proper fenestration.

Islet hypovascularization causes intraislet hypoxia and compensatory metabolic adapatations. As reported by others (26–28), we observed that intraislet hypoxia resulted in increased gene expression of glycolytic enzymes, be it to a limited extent. While hypoxia and the resulting signaling have been claimed to be important for glucose sensing and metabolic control by β-cells (27–33), blood glucose level was only moderately elevated in dTG+DOX mice, even after 25 weeks of *sFLT1* overexpression. Despite subtle differences in expression levels of Glut1/2 and glucokinase, isolated hypovascular islets displayed normal glucose utilization and oxidation profiles, illustrating a remarkable capacity of β-cells to cope with intraislet hypoxia. Nevertheless, our data still attribute an important role to the islet endothelium, since mice with hypovascular islets display a significant decrease of glucose responsiveness of insulin secretion in vivo, contributing to glucose intolerance upon intraperitoneal glucose load. The observed lack of a clear first-phase insulin secretory response of hypovascular islets is likely due to impaired β-cell insulin synthesis and secretion in vivo or to the decreased amount of intraislet vessels, mainly associated with α-cells, leading to a delay in time before glucose can reach the β-cells and for insulin to diffuse to the nearest vessel(s). Moreover, hypoxia-mediated stabilization of HIF1a could additionally explain the observed decrease in glucose-stimulated insulin secretion in vivo as previously reported (26). Of note, hypoxia predominantly affects the second phase of glucose-stimulated insulin secretion in rat and canine islets (30,31); however, this was not observed by us and others, since the second phase of insulin secretion is blunted in mice (34).

In contrast to prenatal *Vegfa* deletion (7–9,11,12), postnatal interference with VEGF-A signaling and subsequent vascular (basement membrane) regression did not influence insulin gene expression, pancreas insulin content, or basal β-cell proliferation rate. As a consequence, the β-cell mass did not differ from control animals. Interestingly, after 25 weeks of *sFLT1* expression, the β-cell size was subtly reduced and an increased amount of small islets with increased α–to–β-cell ratio could be observed. Although further examination is needed, this finding could be attributed to fission of large islets or neoformation of islets (35). While recently it was reported that (*Pdx1* promoter driven) blood vessel ablation promoted pancreatic branching, differentiation, and growth during embryogenesis (4), only minor changes in β-cell size and islet composition were observed after selective ablation of intraislet blood vessels in the adult pancreas in our study. Whether manipulation of the vasculature throughout the entire adult pancreas or more specifically near the ductal epithelium would alter pancreas size or the activation of facultative (endocrine) progenitors remains to be determined. Finally, while signals from activated endothelial cells have been demonstrated to be instrumental for compensatory β-cell proliferation and β-cell mass expansion during pregnancy (36), our data reveal that blood vessels are dispensable for normal, age-dependent augmentation of the β-cell mass and for injury-induced β-cell generation.

Conditional intraislet blood vessel ablation thus enabled clarification of the role of intraislet endothelial cells with regard to adult β-cell function, mass, and proliferation, restricting their importance to proper rapid and adequate glucose-stimulated insulin secretion. The current report could have major implications for design of islet transplantation

protocols. Indeed, efforts are currently undertaken to promote early graft revascularization. Our data, however, indicate that β-cells can survive, function, and even proliferate in a hypovascular and hypoxic state, thereby suggesting that *1*) insufficient vascularization upon transplantation is likely not the predominant cause of early graft loss and *2*) approaches that uniquely promote graft revascularization will likely not result in a major benefit for glycometabolic outcome of islet transplantation.

REFERENCES

1. Lammert E, Cleaver O, Melton D. Induction of pancreatic differentiation by signals from blood vessels. Science 2001;294:564–567
2. Yoshitomi H, Zaret KS. Endothelial cell interactions initiate dorsal pancreas development by selectively inducing the transcription factor Ptf1a. Development 2004;131:807–817
3. Pierreux CE, Cordi S, Hick AC, et al. Epithelial: Endothelial cross-talk regulates exocrine differentiation in developing pancreas. Dev Biol 2010; 347:216–227
4. Magenheim J, Ilovich O, Lazarus A, et al. Blood vessels restrain pancreas branching, differentiation and growth. Development 2011;138:4743–4752
5. Sand FW, Hörnblad A, Johansson JK, et al. Growth-limiting role of endothelial cells in endoderm development. Dev Biol 2011;352:267–277
6. Lammert E, Cleaver O, Melton D. Role of endothelial cells in early pancreas and liver development. Mech Dev 2003;120:59–64
7. Brissova M, Shostak A, Shiota M, et al. Pancreatic islet production of vascular endothelial growth factor—a is essential for islet vascularization, revascularization, and function. Diabetes 2006;55:2974–2985
8. Nikolova G, Jabs N, Konstantinova I, et al. The vascular basement membrane: a niche for insulin gene expression and Beta cell proliferation. Dev Cell 2006;10:397–405
9. Iwashita N, Uchida T, Choi JB, et al. Impaired insulin secretion in vivo but enhanced insulin secretion from isolated islets in pancreatic beta cell-specific vascular endothelial growth factor-A knock-out mice. Diabetologia 2007;50:380–389
10. Kaido T, Yebra M, Cirulli V, Montgomery AM. Regulation of human beta-cell adhesion, motility, and insulin secretion by collagen IV and its receptor alpha1beta1. J Biol Chem 2004;279:53762–53769
11. Lammert E, Gu G, McLaughlin M, et al. Role of VEGF-A in vascularization of pancreatic islets. Curr Biol 2003;13:1070–1074
12. Jabs N, Franklin I, Brenner MB, et al. Reduced insulin secretion and content in VEGF-a deficient mouse pancreatic islets. Exp Clin Endocrinol Diabetes 2008;116(Suppl. 1):S46–S49
13. Milo-Landesman D, Surana M, Berkovich I, et al. Correction of hyperglycemia in diabetic mice transplanted with reversibly immortalized pancreatic beta cells controlled by the tet-on regulatory system. Cell Transplant 2001;10:645–650
14. Nir T, Melton DA, Dor Y. Recovery from diabetes in mice by beta cell regeneration. J Clin Invest 2007;117:2553–2561
15. May D, Gilon D, Djonov V, et al. Transgenic system for conditional induction and rescue of chronic myocardial hibernation provides insights into genomic programs of hibernation. Proc Natl Acad Sci USA 2008;105: 282–287
16. Martín F, Andreu E, Rovira JM, et al. Mechanisms of glucose hypersensitivity in beta-cells from normoglycemic, partially pancreatectomized mice. Diabetes 1999;48:1954–1961
17. Xu X, D'Hoker J, Stangé G, et al. Beta cells can be generated from endogenous progenitors in injured adult mouse pancreas. Cell 2008;132: 197–207
18. Mellitzer G, Bonné S, Luco RF, et al. IA1 is NGN3-dependent and essential for differentiation of the endocrine pancreas. EMBO J 2006;25:1344–1352
19. Chintinne M, Stangé G, Denys B, et al. Contribution of postnatally formed small beta cell aggregates to functional beta cell mass in adult rat pancreas. Diabetologia 2010;53:2380–2388
20. McDonald DM, Choyke PL. Imaging of angiogenesis: from microscope to clinic. Nat Med 2003;9:713–725
21. Miki T, Minami K, Shinozaki H, et al. Distinct effects of glucose-dependent insulinotropic polypeptide and glucagon-like peptide-1 on insulin secretion and gut motility. Diabetes 2005;54:1056–1063
22. De Vos A, Schuit FC, Malaisse WJ. Preferential stimulation by glucose of its oxidation relative to glycolysis in purified insulin-producing cells. Biochem Int 1991;24:117–121
23. Hodgkiss RJ. Use of 2-nitroimidazoles as bioreductive markers for tumour hypoxia. Anticancer Drug Des 1998;13:687–702
24. Granot Z, Swisa A, Magenheim J, et al. LKB1 regulates pancreatic beta cell size, polarity, and function. Cell Metab 2009;10:296–308
25. Bonner-Weir S. Morphological evidence for pancreatic polarity of beta-cell within islets of Langerhans. Diabetes 1988;37:616–621
26. Zehetner J, Danzer C, Collins S, et al. PVHL is a regulator of glucose metabolism and insulin secretion in pancreatic beta cells. Genes Dev 2008;22: 3135–3146
27. Cantley J, Selman C, Shukla D, et al. Deletion of the von Hippel-Lindau gene in pancreatic beta cells impairs glucose homeostasis in mice. J Clin Invest 2009;119:125–135
28. Choi D, Cai EP, Schroer SA, Wang L, Woo M. Vhl is required for normal pancreatic β cell function and the maintenance of β cell mass with age in mice. Lab Invest 2011;91:527–538
29. Ohta M, Nelson D, Nelson J, Meglasson MD, Erecińska M. Oxygen and temperature dependence of stimulated insulin secretion in isolated rat islets of Langerhans. J Biol Chem 1990;265:17525–17532
30. Dionne KE, Colton CK, Yarmush ML. A microperifusion system with environmental control for studying insulin secretion by pancreatic tissue. Biotechnol Prog 1991;7:359–368

31. Dionne KE, Colton CK, Yarmush ML. Effect of hypoxia on insulin secretion by isolated rat and canine islets of Langerhans. Diabetes 1993;42:12–21
32. Kühtreiber WM, Lanza RP, Beyer AM, Kirkland KS, Chick WL. Relationship between insulin secretion and oxygen tension in hybrid diffusion chambers. ASAIO J 1993;39:M247–M251
33. Cheng K, Ho K, Stokes R, et al. Hypoxia-inducible factor-1alpha regulates beta cell function in mouse and human islets. J Clin Invest 2010;120:2171–2183
34. Maechler P, Gjinovci A, Wollheim CB. Implication of glutamate in the kinetics of insulin secretion in rat and mouse perfused pancreas. Diabetes 2002;51(Suppl. 1):S99–S102
35. Miller K, Kim A, Kilimnik G, et al. Islet formation during the neonatal development in mice. PLoS ONE 2009;4:e7739
36. Johansson M, Mattsson G, Andersson A, Jansson L, Carlsson PO. Islet endothelial cells and pancreatic beta-cell proliferation: studies in vitro and during pregnancy in adult rats. Endocrinology 2006;147:2315–2324